

Supplementary Information

Non-Enzymatic-Browning-Reaction: A Versatile Route for Production of Nitrogen-Doped Carbon Dots with Tunable Multicolor Luminescent Display

Weili Wei, Can Xu, Li Wu, Jiasi Wang, Jinsong Ren, and Xiaogang Qu*

Laboratory of Chemical Biology, Division of Biological Inorganic Chemistry, State Key Laboratory of Rare Earth Resource Utilization, Changchun Institute of Applied Chemistry, Graduate School of the Chinese Academy of Sciences, Chinese Academy of Sciences Changchun, Jilin 130022, China

*Correspondence and requests for materials should be addressed to X. Qu (xqu@ciac.jl.cn)

Experimental Section

Materials. The amino acids including tryptophan (Trp), tyrosine (Tyr), phenylalanine (Phe), arginine (Arg), lysine (Lys), histidine (His), glutamic acid (Glu), glutamine (Gln), aspartic acid (Asp), asparagine (Asn), glycine (Gly), alanine (Ala), valine (Val), leucine (Leu), isoleucine (Ile), serine (Ser), threonine (Thr), proline (Pro) and glucose were purchased from Sigma-Aldrich (Steinheim, Germany). All other reagents were of analytical reagent grade. All aqueous solutions were prepared using ultra-pure water (18.2 M Ω cm⁻¹, Milli-Q, Millipore).

Microchip operations. For a typical microchip we used, it consists of two components: polydimethylsiloxane (PDMS) layer with the patterns or stripes and the glass substrate. The microchip was fabricated by using traditional standard soft lithography techniques.[S1] In brief, a silicon wafer was pre-cleaned by H₂SO₄: 30% H₂O₂ (3:1, v/v) and then coated with the negative photoresists SU-8 2050 (2000 rpm, 60 μ m thick film). This silicon wafer was prebaked at 85 °C for 10 min, and then exposed by UV light under the photomask. Further, the patterned microstructure can be generated by developing solution. After hard-baked for 10 min, the master was silanized over night by tridecafluoro-1,1,2,2-tetrahydrooctyl trichlorosilane vapor. PDMS prepolymer and curing agent (10:1) was premixed and poured onto the master. After degassed in a vacuum chamber, the PDMS replicas were cured in an 85 °C oven for 3 h. Finally, the PDMS was peeled from the master and connection holes were made by using a needle. The PDMS layer was cleaned with CH₃OH and H₂O, and sealed with glass slide by oxygen plasma (PDC-32g, Harrick Plasma, Ithaca, NY, USA) treatment for 90 s. PDMS chips were rinsed and cleaned with 70% ethanol for further experiments. The micropatterns in the PDMS chips were loaded with different C-dot-embedded agarose gels (kept as liquid before loading) with a Hamilton syringe.

The MTT assay of cell viability. HeLa cells (in DMEM medium) were dispersed in 96-well plates (90 μ L in each well containing 1×10^4 cells per well). 10 μ L of the C-dots solution with different concentration (0.2, 1, and 2 mg mL⁻¹) was added to each well. Incubation was carried out for 24 h in a humidified atmosphere at 37 °C with 5% CO₂. The cytotoxicity of the C-dots was evaluated by the MTT (3-(4,5-dimethylthiazol-2-yl)-2,5-diphenyltetrazolium bromide) assay. The assay was based on the accumulation of dark blue formazan crystals inside living cells after exposure to MTT, which is well-established for assessment of cellular viability. The destruction of cell membranes by the addition of sodium dodecylsulfate (SDS) resulted in the liberation and solubilization of the crystals. The number of viable cells was thus directly proportional to the level of the initial formazan product created. The formazan concentration was finally quantified using a spectrophotometer by measuring the absorbance

at 570 nm (ELISA reader). A linear relationship between cell number and optical density was established, thus allowing an accurate quantification of changes in the rate of cell proliferation.

Synthesis of Folic Acid-Functionalized C-dots: Conjugation of C-dots with folic acid (FA) was achieved according to our previously reported method.[S2] Typically, free FA (10 mg, 0.0227 mmol) was firstly dissolved in 4 mL 50 mM MES buffer (pH 6.0). The solution of FA was then mixed with a 2 mL aqueous solution of (EDC) (0.068 mmol) and sulfo-NHS (0.068 mmol). After agitating overnight at temperature in the dark, the solution of C-dots (containing 20 mg C-dots) was added to the mixture. The resulting solution was stirred at room temperature for 24 hr and then dialyzed (3000 kD tubing) for 24 h to remove excess FA.

Cell Imaging. Human epithelial cervical cancer cells (Hela cell) were cultured (37 °C, 5% CO₂) on cover glass in Dulbecco's modified Eagle's medium (DMEM) with 10% heat-inactivated fetal bovine serum (FBS) and antibiotics (100 µg/ml streptomycin and 100 U/mL penicillin) overnight. For fluorescent imaging, Hela cells were fixed with 4% sucrose and 4% paraformaldehyde for 20 min and blocked for 40 min in PBS containing 4% BSA and 0.1% Triton X-100. The fixed Hela cells were washed with PBS containing 0.1% Tween 20 for 3 times. Then the fixed and blocked Hela cells were incubated with C-dots for 4 h, and the C-dots-stained cells were mounted on slides with coverslips fluorescent imaging.

Quantum yield (QY) measurements. Fluorescence quantum yields (QYs) of each carbon dot were measured according to the standard method[S3] by comparison of the wavelength integrated intensity of the C-dots to that of the standard. The optical density is kept below 0.05 to avoid inner filter effects. The QYs of the C-dots are calculated using following equation:

$$Q = Q_R \frac{I}{I_R} \frac{OD_R}{OD} \frac{n^2}{n_R^2} \quad (S1)$$

where Q is the QY, I is the integrated intensity, OD is the optical density, and n is the refractive index. The subscript R refers to the reference fluorephore of known QY. In this expression it is assumed that the C-dot and reference are excited at the same wavelength. The observed fluorescence spectra were corrected for nonlinear instrument response before the integration of their total intensities for the calculation of QYs. The quinine sulfate in 0.1 M H₂SO₄ (λ_{ex} =350 nm, QY=0.577) and Rhodamine 101 in ethanol (λ_{ex} =460 nm, QY=1) were used as fluorescence standards. The quinine sulfate was used as standard for the blue and green emission C-dots, and Rhodamine 101 was used for the yellow and orange C-dots. The

refractive indexes of dilute quinine sulfate in 0.1 M H₂SO₄ and Rhodamine 101 in ethanol were 1.333 and 1.362, respectively. All the C-dots aqueous solutions were assumed as water with refractive indexes of 1.333.

Lipophilicity (Log*P*) measurements. The Log*P* values of the C-dots were measured by the most classical and reliable shake flask method with octanol as the hydrophobic and water as hydrophilic phase.[S4] The equilibrated concentrations of C-dots in octanol (*C*_o) and water (*C*_w) phase were measured by fluorescence spectroscopy. The Log*P* values were calculated as follow:

$$\text{Log}P = \log (C_o / C_w) \quad (\text{S2}).$$

Supplementary Figures

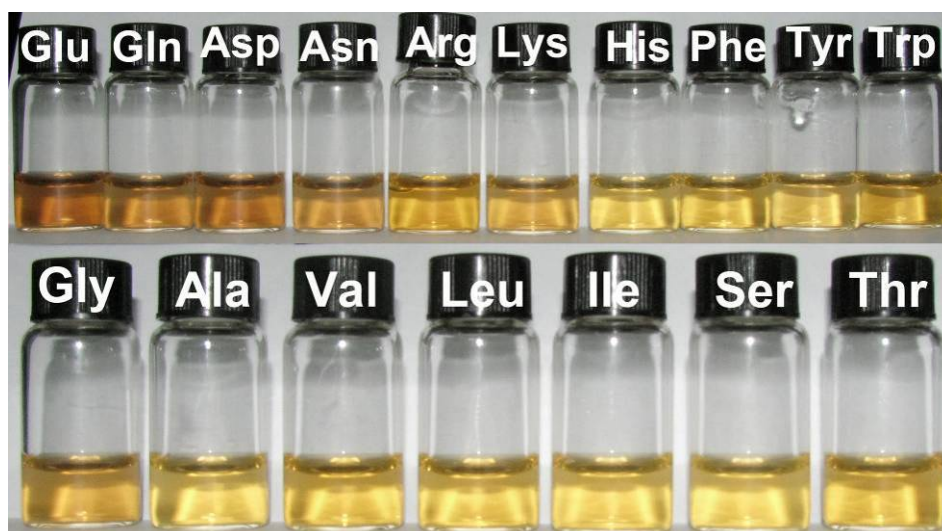


Figure S1 Photograph of the aqueous solutions of the amino acids-derived C-dots (5 mg mL^{-1}). The C-dots derived from glucose and the amino acids Glu, Gln, Asp, Asn, Arg, Lys, His, Phe, Tyr, Trp, Gly, Ala, Val, Leu, Ile, Ser, and Thr were named as Glu-C-dot, Gln-C-dot, Asp-C-dot, Asn-C-dot, Arg-C-dot, Lys-C-dot, His-C-dot, Phe-C-dot, Tyr-C-dot, Trp-C-dot, Gly-C-dot, Ala-C-dot, Val-C-dot, Leu-C-dot, Ile-C-dot, Ser-C-dot, and Thr-C-dot, respectively.

As can be seen from the photograph, Glu-C-dot, Gln-C-dot, Asp-C-dot, and Asn-C-dot solutions exhibit dark brown and the others appeared yellow color. The different color could implicate different optical and physicochemical properties of the C-dots, as evidenced in this work.

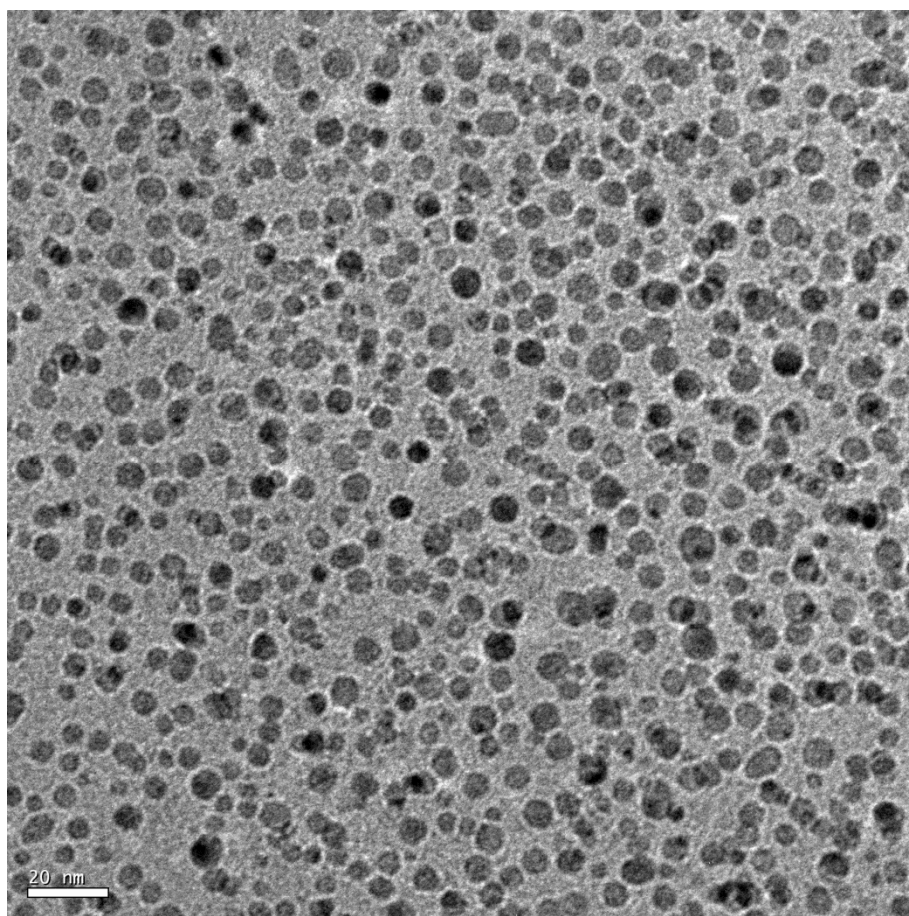


Figure S2 Normal TEM image of Trp-C-dots.

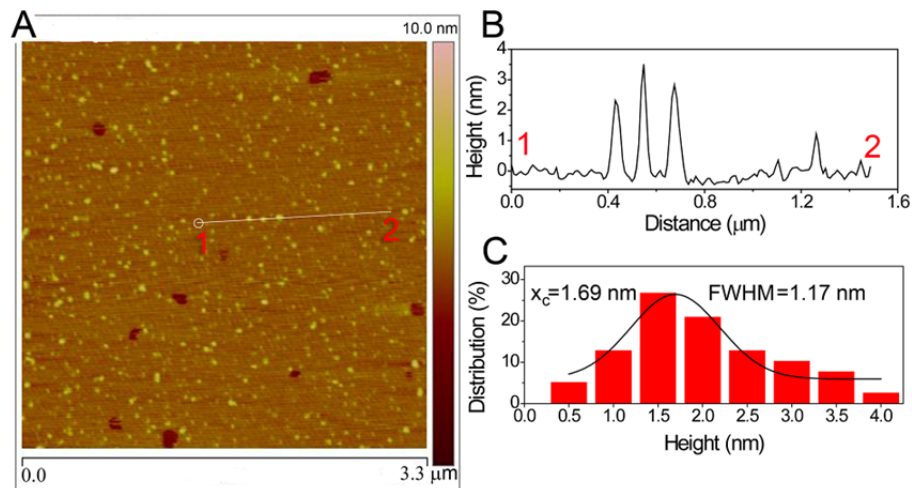


Figure S3 (A) AFM image of Arg-C-dots on a mica substrate. (B) Height profile along the line in (A). (C) Height distribution of Arg-C-dots measured by AFM. The average height of was statistically calculated to 1.69 nm.

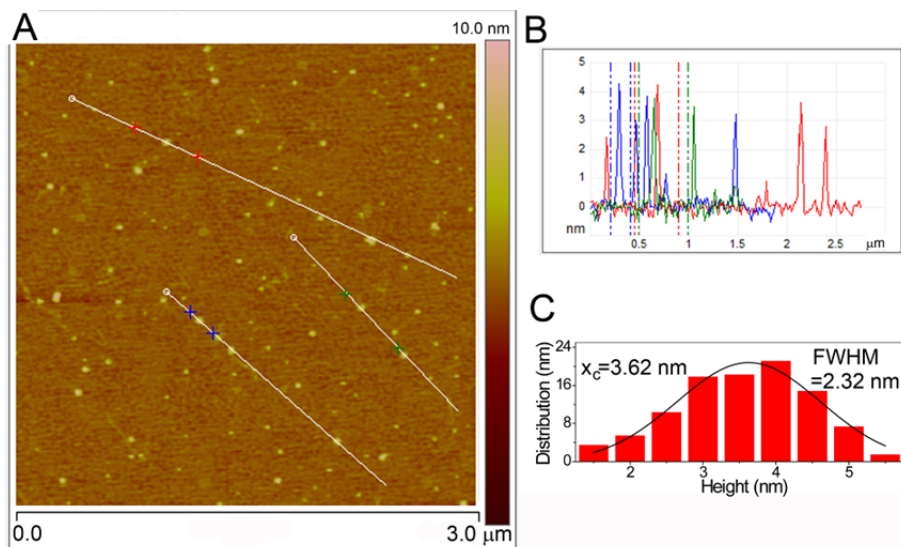


Figure S4 (A) AFM image of Leu-C-dots on a mica substrate. (B) Height profile along the line in (A). (C) Height distribution of Leu-C-dots measured by AFM. The average height of was statistically calculated to 3.62 nm.

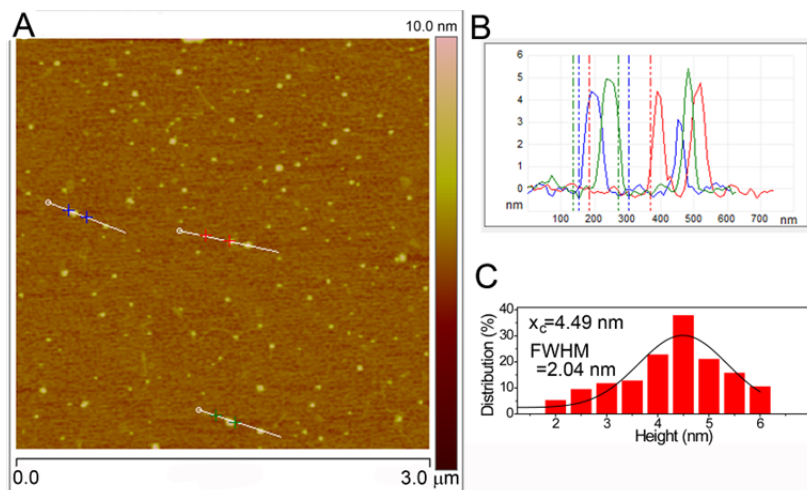


Figure S5 (A) AFM image of Asp-C-dots on a mica substrate. (B) Height profile along the line in (A). (C) Height distribution of Asp-C-dots measured by AFM. The average height of was statistically calculated to 4.49 nm.

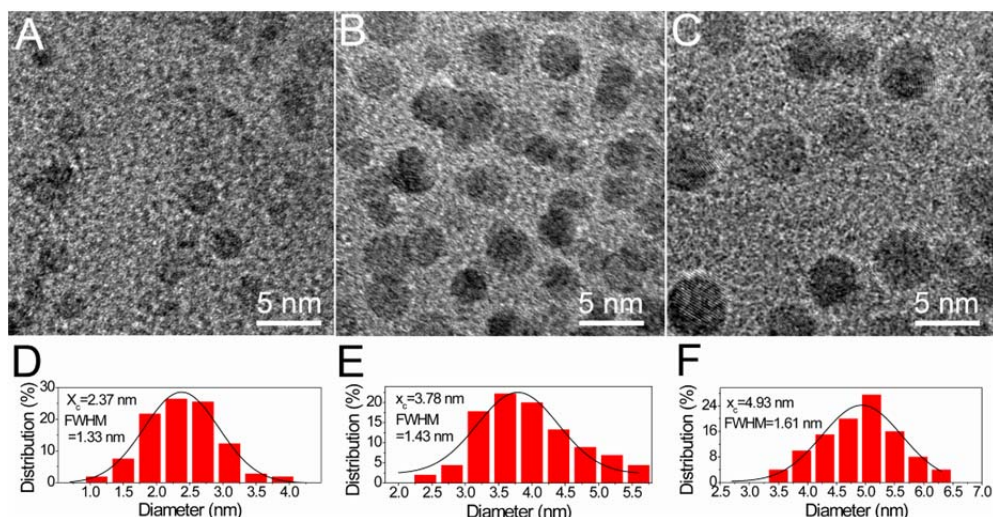


Figure S6 TEM images and diameter distributions of Arg-C-dot (A, D), Leu-C-dot (B, E), and Asp-C-dot (C, F).

The results of AFM and TEM measurement are in well consistent. In addition to the size distribution, the TEM images also revealed that, the C-dots became less crystallized with a decrease of size. E.g., the lattice structure can hardly be observed in TEM image of Arg-C-dots. This could be attributed to the ultra-small C-dots that were only composed of little number of atoms (such as C, N, and O). The limited atoms were not enough to form ordered crystalline structure.

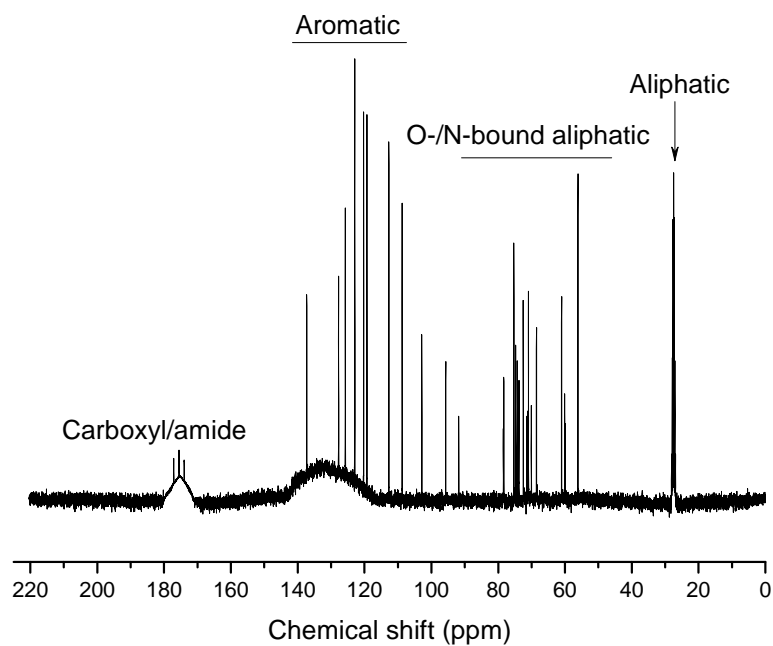


Figure S7 ^{13}C NMR spectrum of Trp-C-dots. The ^{13}C NMR spectrum was recorded in a D_2O solution at 25 °C on a Bruker Avance 600 MHz NMR Spectrometer.

With respect to ^{13}C NMR, the peaks between 170 and 180 ppm are due to carbons in the carboxylic/carbonyl/amide bonds; the series peaks within the range of 100 to 140 ppm are ascribed to aromatic carbons; the peaks from 50 to 80 ppm to O- and N-bound aliphatic carbons; and the peaks near 25 ppm to methylene carbons.

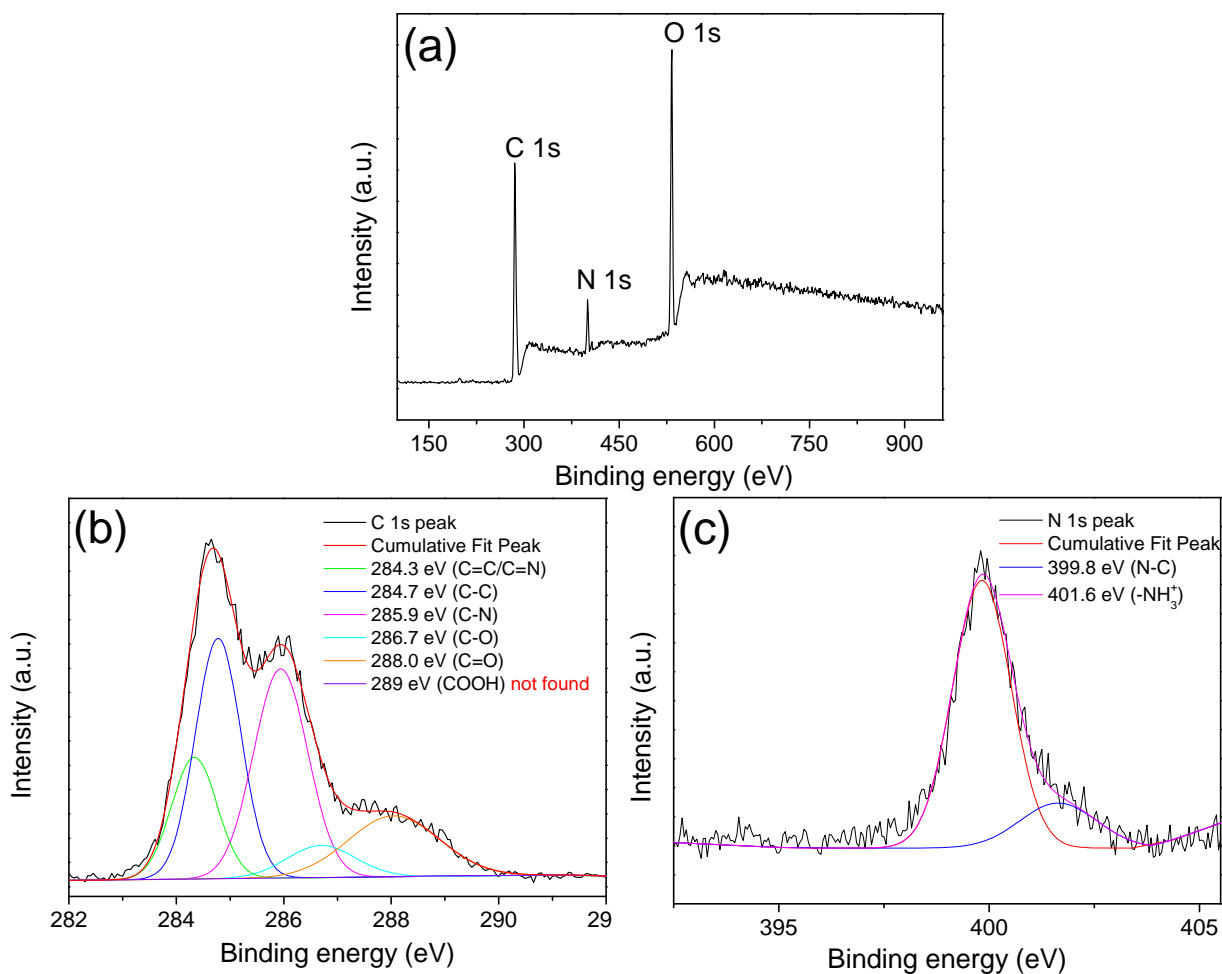


Figure S8 (a) XPS spectrum of the as-prepared Arg-C-dot. (b, c) High-resolution C 1s (b) and N 1s (c) peaks of Arg-C-dot.

According to the XPS spectra, the peak of amino group (in $-\text{NH}_3^+$ form) was found at 401.6 eV. This result is reasonable due to the excess of amino groups in the starting materials. On the other hand, signal for carboxyl groups was very weak. The composition of Lys-C-dot is similar to Arg-C-dot.

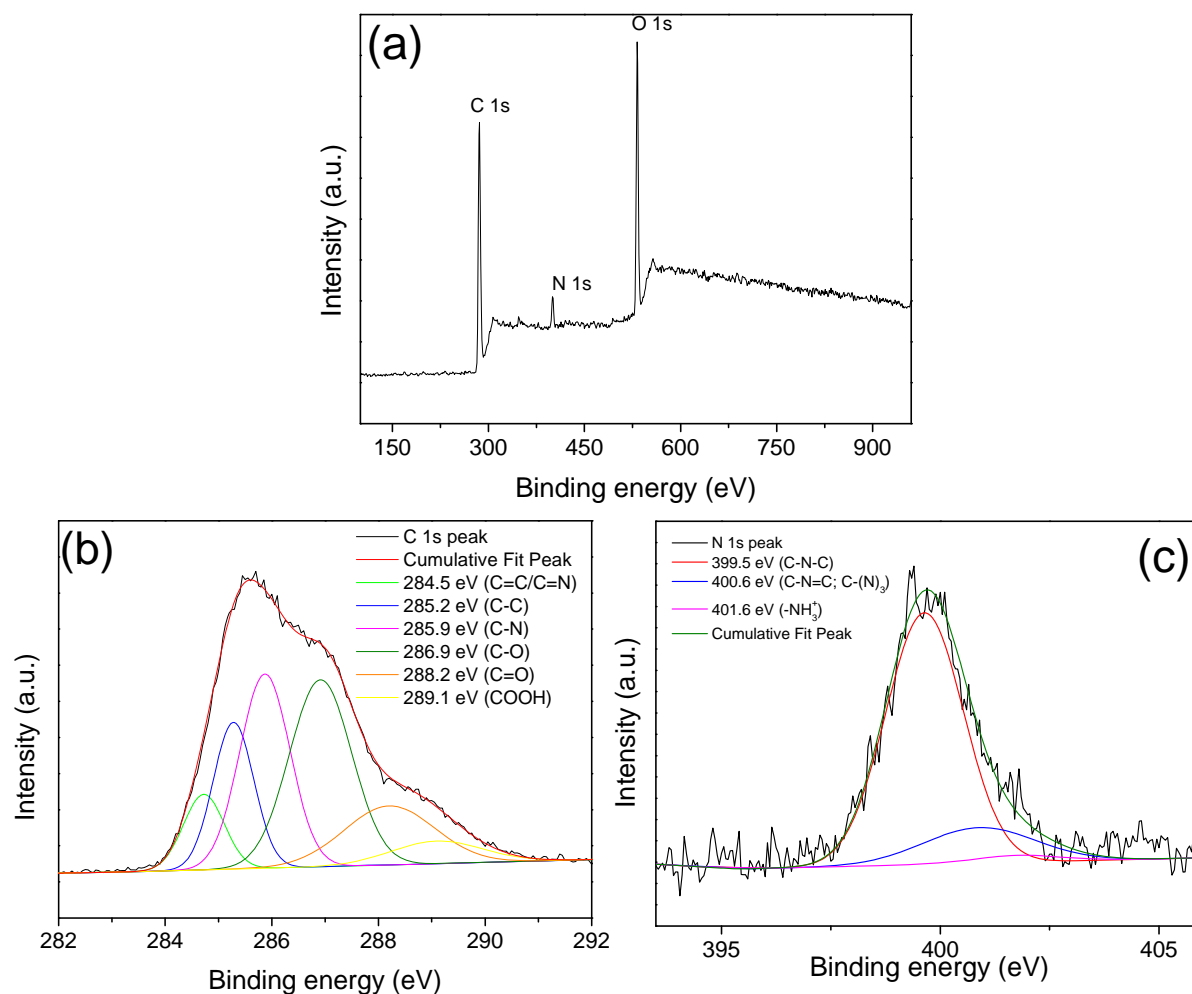


Figure S9 (a) XPS spectrum of the as-prepared Leu-C-dot. (b, c) High-resolution C 1s (b) and N 1s (c) peaks of Leu-C-dot.

Accordingly, N atoms were successfully incorporated into Leu-C-dot. But the content of N in Leu-C-dot is relatively lower than in the basic amino acids derived C-dots (e.g. Arg-C-dot). The N/C atom ration in Leu-C-dot is 7.69%, which is much smaller than that of Arg-C-dot (15.35%). The values were calculated from XPS spectra.[S5] Therefore, although doping N atoms might cause blue shift of the emission, the Leu-C-dot still emits green color fluorescence. In addition, carboxyl groups were found on Leu-C-dot surface, which allowing further functionalization. The other neutral aliphatic amino acids-derived C-dots (see as Table S1) were similar to Leu-C-dot. Note that, amino groups still exist in these kinds of C-dots with a low content.

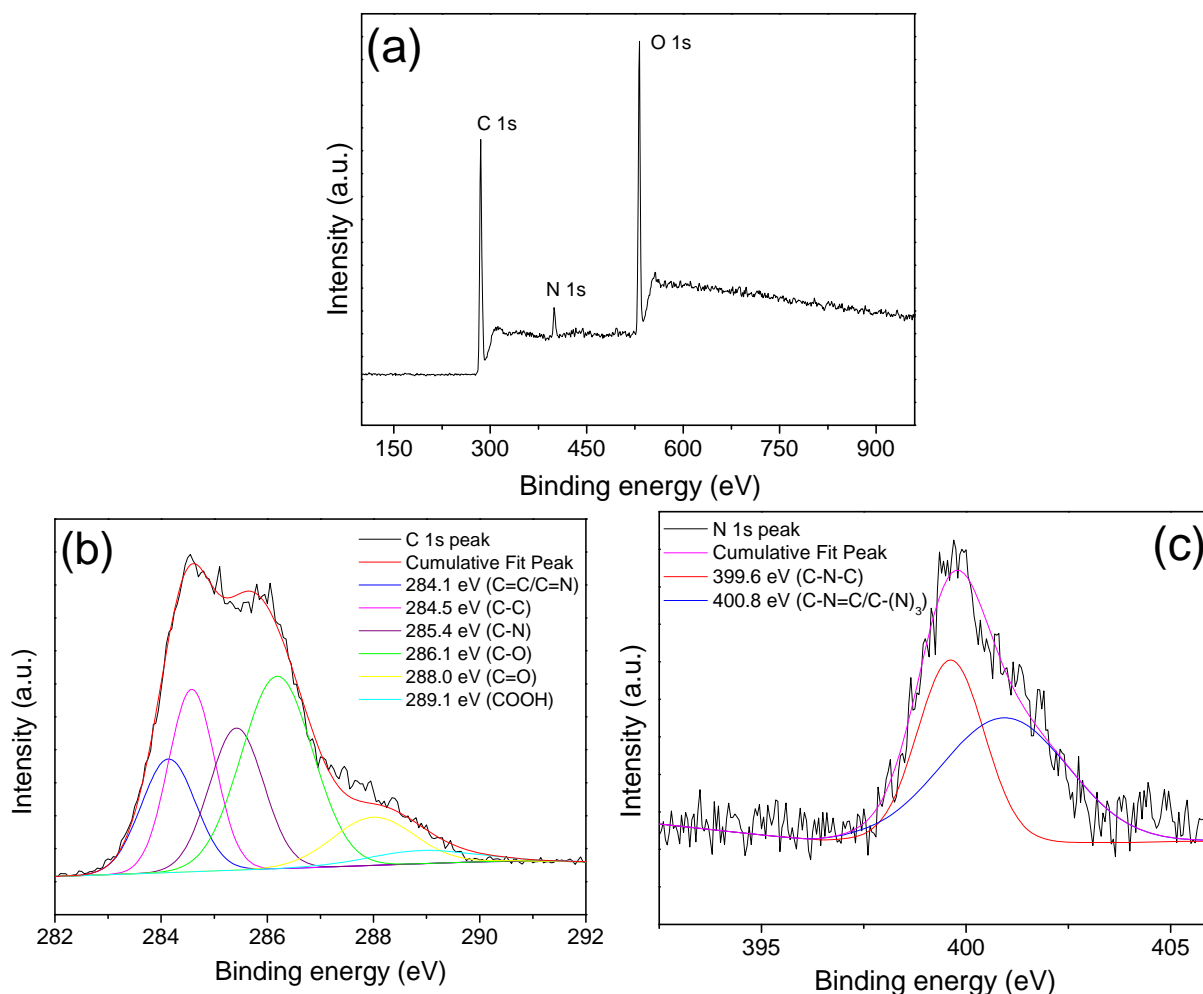


Figure S10 (a) XPS spectrum of the as-prepared Asp-C-dot. (b, c) High-resolution C 1s (b) and N 1s (c) peaks of Asp-C-dot.

Obviously, large amount of carboxyl groups were found in the surface of Asp-C-dot (XPS peak at 289.1 eV). Interestingly, the composition of Asp-C-dot is similar to the graphene oxide which also possesses lots of carboxyl groups and emits long wavelength fluorescence (from red to near infrared).[S6] Hence it is reasonable that the Asp-C-dot shows yellow to orange (relative longer emission wavelength than other C-dots) emission color. The Glu-C-dot, Asn-C-dot, and Gln-C-dot are similar to Asp-C-dot.

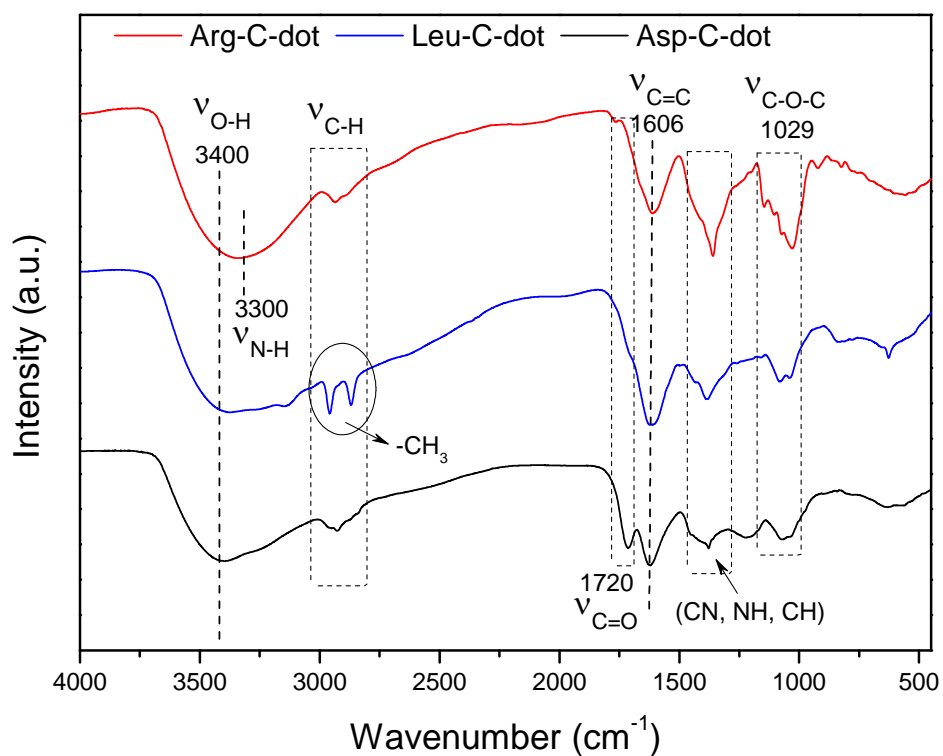


Figure S11 FTIR spectra of Arg-C-dot, Leu-C-dot, and Asp-C-dot. From the spectra, Arg-C-dot possesses amino groups, Asp-C-dot possesses a lot of carboxyl groups, and methyl groups are found for Leu-C-dots. The FTIR and XPS results are in well accordance.

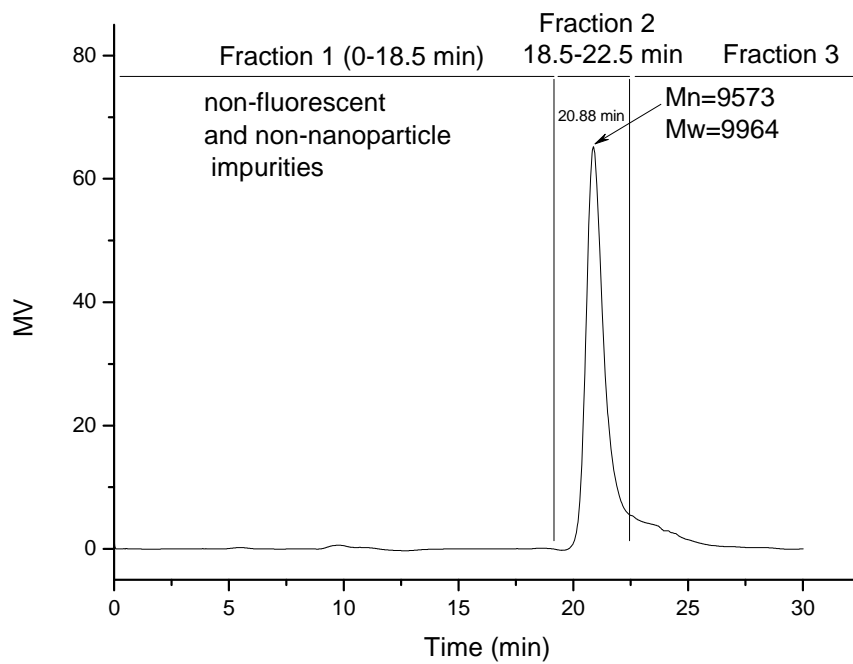


Figure S12 GPC chromatogram of Trp-C-dots. Trp-C-dots were prepared as water solution. The measurement was carried out with Waters 2414 System equipped with UltrahydrogelTM linear column and a Waters 2414 refractive index detector. Injection volume= 200 μ L.

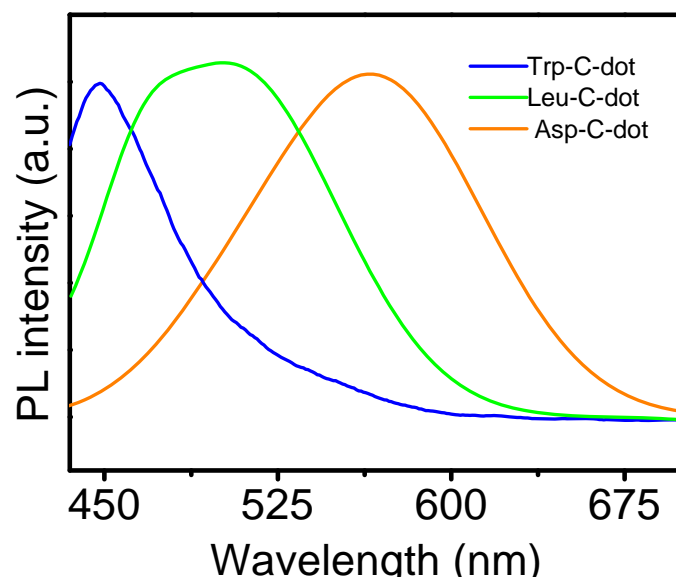


Figure S13 PL emission spectra of Trp-C-dot , Leu-C-dot, and Asp-C-dot. Excitation=430 nm. The three C-dots shows different emission color.

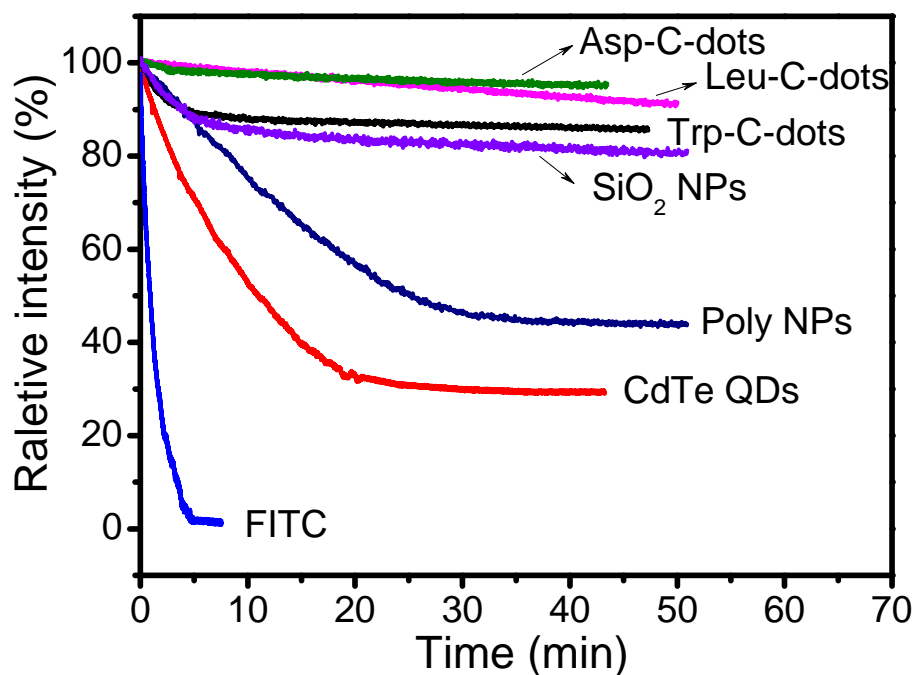


Figure S14 Photostability comparison of FITC, CdTe QDs, polymer nanoparticles (Poly NPs), dye doped silica nanoparticles (SiO₂ NPs) and as-prepared C-dots. The FITC (fluorescein isothiocyanate) is one of the most widely used fluorescent dyes, and CdTe QDs are generally recognized as photostable fluorescent labels.

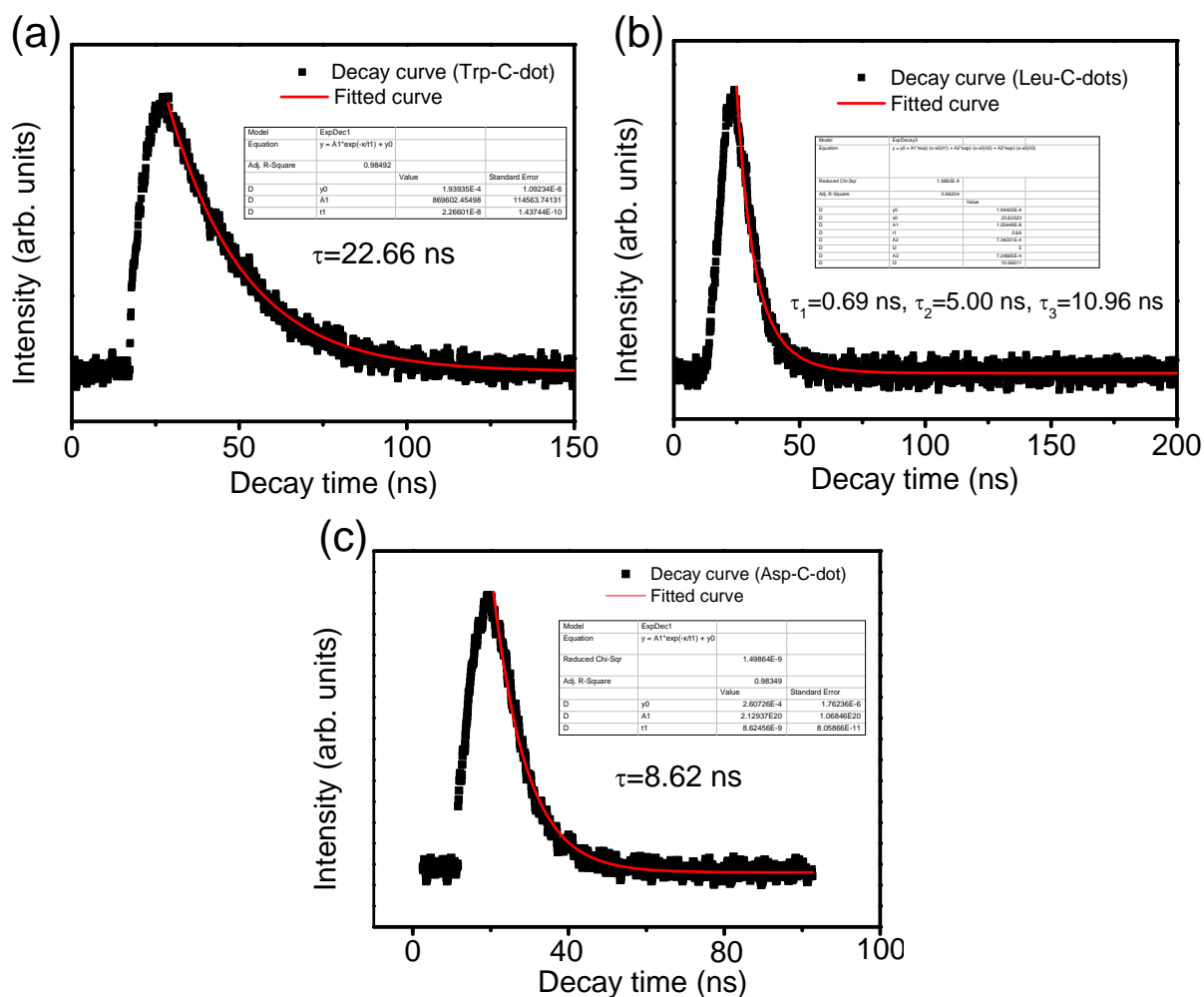


Figure S15 Luminescence decay curves of Trp-C-dot (excitation=355 nm, monitored at 450 nm), Leu-C-dot (excitation=355 nm, monitored at 520 nm), and Asp-C-dot (excitation=405 nm, monitored at 575 nm).

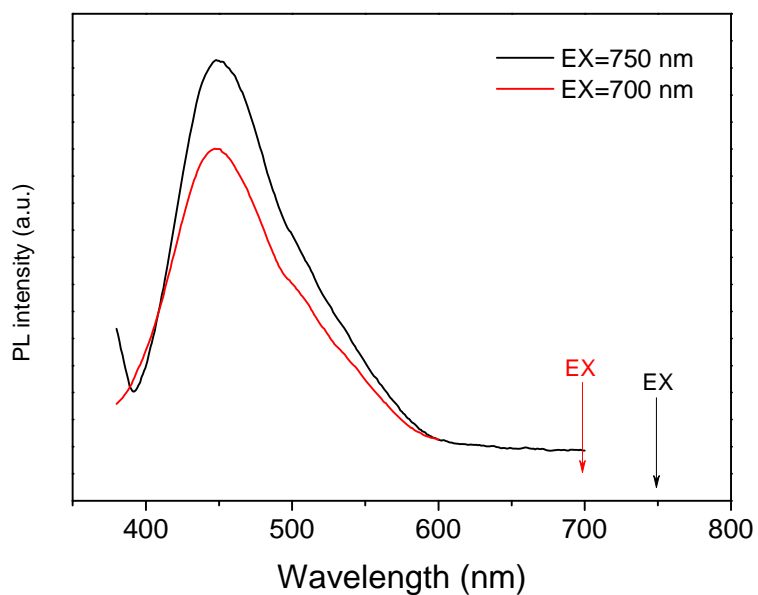


Figure S16 Upconverting fluorescent spectra of Trp-C-dots. The spectra were measured by a JASCO FP-6500 spectrofluorometer with the slit width for the excitation and emission of 5 nm. This property is very important for myriad applications such as multi-photon bioimaging. The other C-dots all have similar upconverting properties.

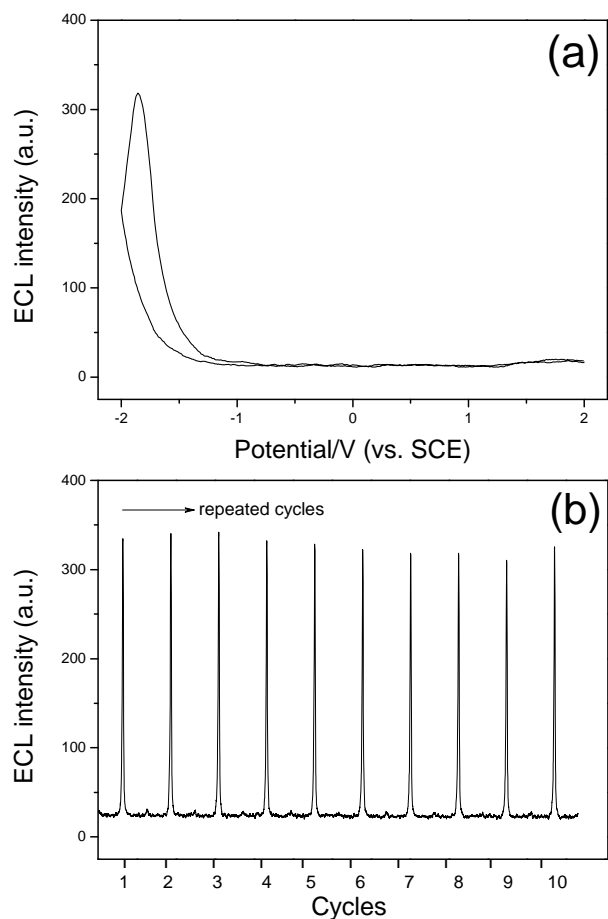


Figure S17 (a) Electrochemiluminescence (ECL)-potential curve of Trp-C-dot modified electrode at a scan rate of 50 mV S^{-1} . (b) ECL of Trp-C-dot under each potential scanning. The $\text{Na}_2\text{S}_2\text{O}_8$ was used as ECL coreactant.[S7] The ECL emission was detected with a Model MPI-A Electrochemiluminescence Analyzer with a conventional three-electrode system composed of a platinum wire as the auxiliary electrode and a saturated calomel electrode (SCE) as the reference; working electrodes were bare Glassy carbon electrode (GCE 4 mm diameter).

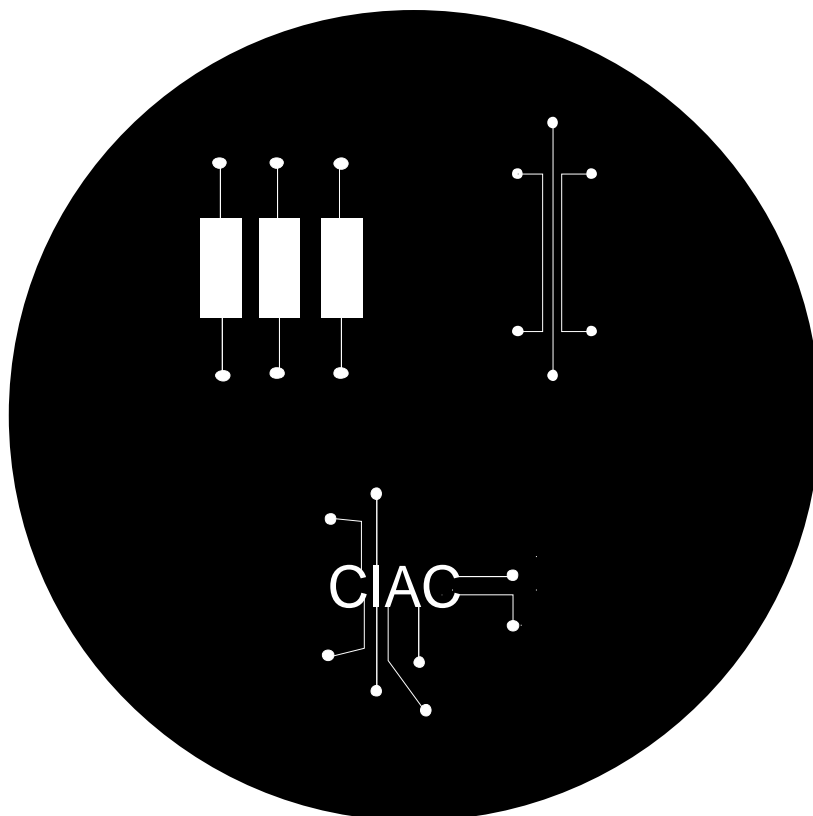


Figure S18 The microchip-based patterns. The patterns were designed in the software Adobe Illustrator CS4.

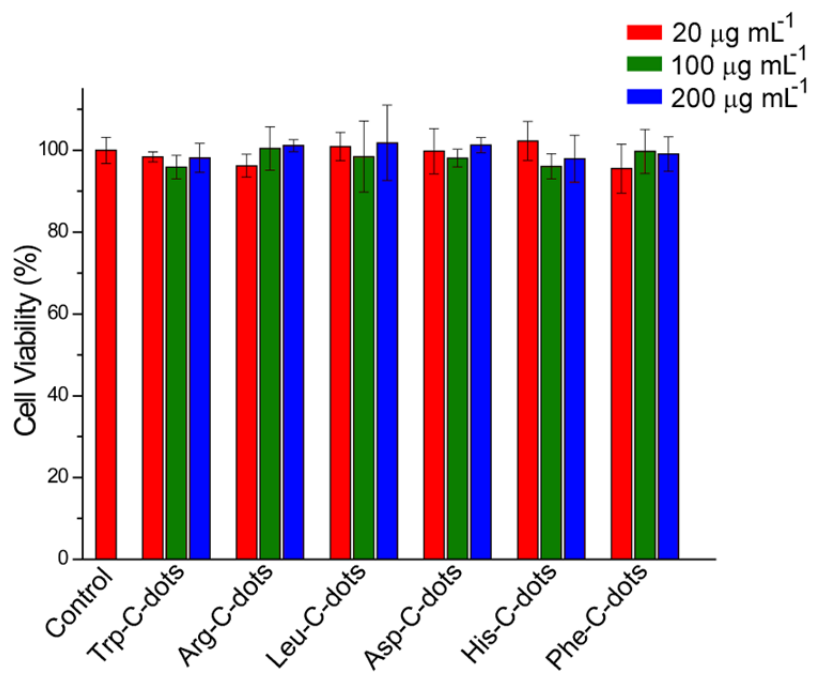
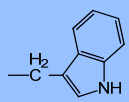
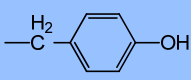
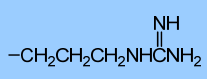
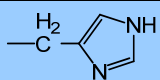


Figure S19 Cell viability assay with HeLa cells (one typical kind of cervical cancer cells) treated with different C-dots for 24 h.

Supplementary Tables

Table S1. Natural amino acids that was used for the synthesis of C-dots.

Name	Side chains (R)	Category*	Name	Side chains (R)	Category*
Tryptophane (Trp)		Ar	Glycine (Gly)	-H	N
Tyrosine (Tyr)		Ar	Alanine (Ala)	-CH ₃	N
Phenylalanine (Phe)	-CH ₂ Ph	Ar	Valine (Val)	-CH(CH ₃) ₂	N
Arginine (Arg)		B	Leucine (Leu)	-CH ₂ CH(CH ₃) ₂	N
Lysine (Lys)	-CH ₂ CH ₂ CH ₂ CH ₂ NH ₂	B	Isoleucine (Ile)	-CH(CH ₃)C ₂ H ₅	N
Histidine (His)		B	Serine (Ser)	-CH ₂ OH	N
Glutamic acid (Glu)	-CH ₂ CH ₂ COOH	A	Threonine (Thr)	-CH(CH ₃)OH	N
Glutamine (Gln)	-CH ₂ CH ₂ CONH ₂	A	Proline (Pro)	-CH ₂ CH ₂ CH ₂ CH ₂ -	Not used
Aspartic acid (Asp)	-CH ₂ COOH	A	Cystein (Cys)	-CH ₂ SH	Not used
Asparagine (Asn)	-CH ₂ CONH ₂	A	Methionine (Met)	-CH ₂ CH ₂ SCH ₃	Not used

*The amino acids were classified by the side chains:

“N” referred as neutral aliphatic amino acids;

“A” referred as acidic amino acids and corresponding amides;

“B” referred as basic amino acids;

“Ar” referred aromatic amino acids.

The two S-containing amino acids Met and Cys were not used due to the release of smelly by-products during the synthesis. Proline (Pro) was not used because it lacks of primary amine, which initiates the Maillard reaction with glucose.

Table S2. Average size, physicochemical and emission properties of the amino acid derived C-dots.

C-dots	Average size (nm)		Composition (wt %)				Zeta potential (mV)	Log <i>P</i>	QY (%)	QY _{ab} ^d (%)	Emission color
	Height ^a	Diameter ^b	C	N	O	H ^c					
Trp-C-dot	2.77	2.88	50.70	7.28	37.31	4.71	-10.2	0.22	69.1	68.6	Blue
Try-C-dot	2.96	3.23	54.12	3.12	36.60	6.16	-5.3	-0.15	42.5	43.7	Blue
Phe-C-dot	3.08	3.35	55.87	3.23	35.62	5.28	-7.3	0.16	39.7	40.5	Blue
Arg-C-dot	1.69	2.37	49.06	8.80	35.45	6.69	+37.2	-2.33	50.2	46.3	Blue
Lys-C-dot	1.62	2.24	50.29	6.32	33.33	10.0	+28.5	-2.18	53.4	51.7	Blue
His-C-dot	2.23	2.72	51.32	8.18	37.90	2.60	+32.5	-2.52	48.7	49.6	Blue
Leu-C-dot	3.62	3.78	55.67	3.15	32.52	8.66	-8.9	0.23	53.6	51.9	Green
Gly-C-dot	3.48	3.86	61.12	4.23	28.62	6.03	-11.3	-2.67	44.2	45.8	Green
Ala-C-dot	3.53	3.49	60.08	3.46	26.88	9.58	-15.1	-3.02	32.3	38.4	Green
Val-C-dot	3.66	3.87	61.98	2.82	27.17	8.03	-16.2	-2.13	33.5	37.9	Green
Ile-C-dot	3.22	3.45	59.65	2.42	28.41	9.52	-9.3	0.22	40.1	46.2	Green
Ser-C-dot	3.75	3.92	52.58	3.55	33.46	10.4	-13.2	-2.54	34.2	39.7	Green
Thr-C-dot	2.98	3.24	55.39	3.63	32.98	8.00	-14.5	-2.63	41.3	42.5	Green
Asp-C-dot	4.49	4.93	53.26	3.28	36.76	6.70	-45.1	-3.12	35.8	34.5	Yellow-t o-Orange
Asn-C-dot	3.98	4.21	60.2	4.65	28.3	6.85	-20.2	-2.13	31.9	33.2	Yellow-t o-Orange
Glu-C-dot	4.92	5.12	55.9	3.12	35.7	5.28	-39.3	-3.05	30.2	31.7	Yellow-t o-Orange
Gln-C-dot	4.23	4.52	54.56	4.55	29.9	9.99	-22.4	-2.67	33.5	35.6	Yellow-t o-Orange

^a The height was measured by AFM;

^b The diameter was measured by TEM;

^c The content of H was calculated against the determined C, O and N values.

^d The QY_{ab} values measured with an Absolute PL Quantum Yield Spectrometer (Hamamatsu, C11347-11 Quantaaurus-QY system).

Supplementary References

- S1. Q. Chen, J. Wu, Y. Zhang, J.-M. Lin, *Anal. Chem.* **2012**, *84*: 1695-1701.
- S2. Y. Song, Y. Chen, L. Feng, J. Ren, X. Qu, *Chem. Commun.* **2011**, *47*, 4436-4438.
- S3. J. R. Lakowicz, *Principles of Fluorescence Spectroscopy*, 3rd ed., Springer, New York, **2006** (p77).
- S4. A. Leo, C. Hansch, D. Elkins, *Chem. Rev.* **1971**, *71*: 525-616.
- S5. M. P. Seah, *Surf. Interface Anal.* **1980**, *2*: 222-239.
- S6. C.-T. Chien, S.-S. Li, W.-J. Lai, Y.-C. Yeh, H.-A. Chen, I. S. Chen, L.-C. Chen, K.-H. Chen, T. Nemoto, S. Isoda, M. Chen, T. Fujita, G. Eda, H. Yamaguchi, M. Chhowalla, C.-W. Chen, *Angew. Chem. Int. Ed.* **2012**, *51*, 6662-6666.
- S7. M. Yin, L. Wu, Z. Li, J. Ren, X. Qu, *Nanoscale* 2012, *4*: 400-404.